High-time Resolution Source Apportionment of $PM_{2.5}$ in Beijing with Multiple Models

Yue Liu [1], Mei Zheng [1,*], Mingyuan Yu [1], Xuhui Cai [1], Huiyun Du [2,3], Jie Li [2], Tian Zhou [1], Caiqing Yan [1], Xuesong Wang [1], Zongbo Shi [4,5], Roy M. Harrison [4,6], Qiang Zhang [7], Kebin He [7]

[1] SKL-ESPC and BIC-ESAT, College of Environmental Sciences and Engineering, Peking University, Beijing 100871, China

[2] State Key Laboratory of Atmospheric Boundary Layer Physics and Atmospheric Chemistry, Institute of Atmospheric Physics, Chinese Academy of Sciences, Beijing 100029, China

[3] Center for Excellence in Urban Atmospheric Environment, Institute of Urban Environment, Chinese Academy of Sciences, Xiamen, China

[4] Division of Environmental Health and Risk Management, School of Geography, Earth and Environmental Sciences, University of Birmingham, Edgbaston, Birmingham, B15 2TT, UK

[5] Institute of Surface Earth System Science, Tianjin University, Tianjin, 300072, China

[6] Department of Environmental Sciences / Center of Excellence in Environmental Studies, King Abdulaziz University, PO Box 80203, Jeddah, 21589, Saudi Arabia

[7] State Key Joint Laboratory of Environment Simulation and Pollution Control, School of Environment, Tsinghua University, Beijing 100084, China

Correspondence to: Mei Zheng (mzheng@pku.edu.cn)

Abstract

Beijing has suffered from heavy local emissions as well as regional transport of air pollutants, resulting in severe atmospheric fine particle ($PM_{2.5}$) pollution. This study developed a combined method to investigate source types of $PM_{2.5}$ and its source regions during winter 2016 in Beijing, which include the receptor model (Positive Matrix Factorization, PMF), footprint, and an air quality model. The PMF model was performed with high-time resolution measurements of trace elements, water soluble ions, organic carbon, and elemental carbon using online instruments during the wintertime campaign of the Air

Pollution and Human Health-Beijing (APHH-Beijing) program in 2016. Source types and their contributions estimated by PMF model using online measurement were linked with source regions identified by the footprint model, and the regional transport contribution was estimated by an air quality model (the Nested Air Quality Prediction Model System, NAQPMS) to analyze the specific sources and source regions during haze episodes. Our results show that secondary and biomass burning sources were dominated by regional transport while the coal combustion source increased with local contribution, suggesting that strict control strategies for local coal combustion in Beijing and a reduction of biomass burning and gaseous precursor emissions in surrounding areas were essential to improve air quality in Beijing. The combination of PMF with footprint results revealed that the secondary source was mainly associated with southern footprints (53%). The northern footprint was characterized by a high dust source contribution (11%) while industrial source increased with the eastern footprint (10%). The results demonstrated the power of combining receptor model-based source apportionment with other models in understanding the formation of haze episodes and identifying specific sources from different source regions affecting air quality in Beijing.

Keywords: Source apportionment, multiple models, regional transport

1. Introduction

Presently, haze in China has the characteristics of high frequency and long duration on a regional scale, and has influenced public life and human health (Xie et al., 2016). High concentrations of fine particulates, which can significantly reduce atmospheric visibility, are one of the main factors in the formation of haze episodes (Sun et al., 2016b; Watson et al., 2002; Yang et al., 2015). Previous studies have found that $PM_{2.5}$ can be emitted from various sources, including residential coal combustion, biomass burning, traffic-related sources, industrial source and dust (Gao et al., 2016; Kotchenruther et al., 2016; Taghvaee et al., 2018; Watson et al., 2001; Zong et al., 2016). Therefore, it is important to have a

better understanding of the major source types and their contribution to $PM_{2.5}$ in order to formulate science-based effective policies and regulations.

As the capital of China, Beijing has suffered from heavy emissions from various sources, resulting in severe $PM_{2.5}$ pollution (Li et al., 2017a; Lv et al., 2016). The source apportionment of $PM_{2.5}$ in Beijing has received great attention in recent years, which is mostly based on receptor models (Gao et al., 2016; Li et al., 2017e; Lv et al., 2016; Song et al., 2006; Yang et al., 2016). Receptor models including the Chemical Mass Balance model (CMB) and Positive Matrix Factorization model (PMF) are the most commonly used methods of source apportionment in China, and are implemented by application of mathematical methods to measurements of chemical composition of fine particles at receptor sites (Cooper et al., 1980; Gao et al., 2016; Lv et al., 2016; Zheng et al., 2005). The receptor model can identify and quantify the contribution of multiple source types based on in-situ measurements and specific source tracers. Gao et al. (2016) employed two receptor models, PMF and Multilinear Engine 2 (ME2), to conduct high-time resolution source apportionment of $PM_{2.5}$ in summer in Beijing. The results showed that PMF and ME2 corresponded well with each other, and secondary source was predominant in Beijing (38-39%). Similar source apportionment results were reported by in Peng et al. (2016) with secondary source contributing 35-40%. Sun et al. (2016b) used online instruments and PMF to investigate the rapid evolution of a severe haze episode in winter in Beijing and showed the variation of chemical components during four stages of haze. By conducting receptor models based on high-time resolution online measurement, the source types and source contributions in Beijing have been analyzed in previous studies (Gao et al., 2016; Peng et al., 2016; Song et al., 2006). However, these studies still have limitations in that source apportionment based on receptor models are only restricted to one or several receptor sites without information about detailed source regions as well as the local and regional source contributions.

Previous studies have indicated that $PM_{2.5}$ pollution in Beijing has been significantly influenced by regional transport and meteorological conditions (Han et al., 2015; Li et al., 2017a; Zhao et al., 2013). With the development of the function of source apportionment in air quality models, source regions and

relative contributions to the receptor site could be quantitively estimated, based on emission inventory of pollution sources and meteorological fields (Burr et al., 2011; Kwok et al., 2013; Zhang et al., 2015). Li et al. (2016) found that regional transport highly contributed to the rapid increase stage of $PM_{2.5}$, with the transport height ranged from 200 to 700 m above ground level with application of the Nested Air Quality Prediction Model System (NAQPMS). Han et al. (2018) used a regional air quality modeling system coupling with ISAM (Integrated Source Apportionment Method) and found that air pollutants derived from Hebei and Shandong provinces were major contributors to $PM_{2.5}$ in Beijing, with contributions up to 25% and 10%, respectively. The air quality model has advantages of analyzing spatial distribution and regional transport of pollutants, but it also has large uncertainties due to emission inventory, boundary layer meteorological processes and complex atmospheric chemical processes.

Due to the importance of the regional transport contribution to $PM_{2.5}$ in Beijing, the limitations of receptor models cannot be ignored. The source types and source contribution derived from receptor models can be combined with the contribution and direction of regional transport derived from chemical transport models. In this study, we employed the receptor model (PMF), the air quality model (NAQPMS) and a footprint model simultaneously based on high-time resolution online measurement data to investigate sources and regional transport of $PM_{2.5}$ in Beijing during November to December in 2016, as part of the Air Pollution and Human Health (APHH) campaign. The goal of the study is to link the contribution of different sources by PMF with the source regions by footprint, and the regional transport contribution by NAQPMS. The combination of multiple models gives greater power to identify specific sources and source regions.

2. Materials and methods

2.1 Online measurement of $PM_{2.5}$

Online sampling of $PM_{2.5}$ was conducted from November 2016 to December 2016 in winter, which was within the heating period of Beijing. The sampler was operated at the Peking University monitoring

site (PKU, 39°59′21″N, 116°18′25″E) in the northwestern part of Beijing city. There are no obvious emission sources locally, except two major roads (150 m to the east and 200 m to the south). Situated in a mixed district of teaching, residential, and commercial areas, the sampling site is representative of the Beijing urban area (Liu et al., 2018; Yan et al., 2015). The sampling site is located on the sixth floor of a teaching building within PKU. The inlet of the instrument is about 20 m above the ground.

Online $PM_{2.5}$ mass concentrations were continuously measured using a Tapered Element Oscillating Microbalance (TEOM 1405F, Thermo Fisher Scientific Inc.). Organic carbon (OC) and elemental carbon (EC) were simultaneously monitored by a Semi-continuous OCEC Carbon Aerosol Analyzer (Sunset Laboratory Inc.) with 1-h time resolution. The Sunset OC/EC analyzer uses a modified NIOSH 5040 thermal-optical protocol as its default protocol, which produces a relatively reliable determination of OC, EC, and the OCEC split (Bauer et al., 2009). More detailed information could be found in Bauer et al., 2009.

An in-situ Gas and Aerosol Compositions monitor (IGAC, Model S-611, Fortelice International Co.Ltd.), which could collect both gases and particles simultaneously, was applied to measure water-soluble ions online with 1-h time resolution in this study. A detailed description of IGAC can be found in Young et al. (2016). Briefly, IGAC was composed of three major units, including a Wet Annular Denuder (WAD) to collect gases into aqueous solution, a Scrub and Impact Aerosol Collector (SCI) to collect particles into solution and a sample analysis unit comprised of two ion chromatographs (DionexICS-1000) for analyzing anions and cations (IC). Ambient air was drawn through a PM_{10} inlet followed by a $PM_{2.5}$ cyclone at a flow rate of 16.7 L min^{-1}, and then gases and $PM_{2.5}$ were separately collected by WAD and SCI. Both gaseous and aerosol samples were injected into 10 mL glass syringes which were connected to the IC for analysis (30-min time resolution for each sample). The concentrations of eight water-soluble inorganic ions (e.g., NH_4^+, Na^+, K^+, Ca^{2+}, Mg^{2+}, SO_4^{2-}, NO_3^- and Cl^-) in the fine particles were measured.

Twenty-three trace elements in $PM_{2.5}$ were measured by an Xact 625 Ambient Metal Monitor (Cooper Environmental Services LLC, USA) with 1-h time resolution. Among them twelve elements (e.g.,

K, Ca, Ba, Cr, Mn, Fe, Cu, Ni, Zn, As, Se, Pb) were selected for further analysis, while other trace elements (such as V, Co, Tl) were not used here due to the low concentrations (below the method detection limit). The ambient air was sampled on a Teflon filter tape inside the instrument through a $PM_{2.5}$ cyclone inlet at a constant flow rate of 16.7 L min^{-1}, and then the sample was automatically analyzed by nondestructive energy-dispersive X-ray fluorescence (XRF) to determine the mass of the species. This instrument has been documented with Environment Technology Verification (ETV) and certified by the US Environment Protection Agency (EPA, 2012). The detection limit of each species measured by the online instruments could be seen in Table S1.

Strict quality assurance (QA) and quality control (QC) protocols for online instruments were performed during the whole sampling period. For IGAC, the internal standard (LiBr) was added continuously to each sample and analyzed by the IC system during the analysis to check the stability of the IGAC instrument. During the sampling period, the mean concentrations of Li^+ and Br^- were within the range of three standard deviations, suggesting a stable condition of the IGAC (see Fig. S1). As shown in Fig. S2, the slope of the linear fitting between the anions and cations was 0.93, and R^2 was 0.96. As for the OC/EC analyzer, external standard calibration using the stock sucrose solution was conducted before operation to calibrate carbon analysis. For the Xact, a Pd rod was used as automatic internal quality control to check the performance of the instrument on a daily basis (see Fig. S3). Additionally, a QA energy calibration test and QA energy level test were performed for a half hour after midnight every day to monitor any possible shift and instability of the XRF. During our field campaign, the Xact remained stable and reliable.

Chemical closure has been done between the measured and reconstructed $PM_{2.5}$. Organic matter (OM) was calculated as OM= 1.6 ×OC (Turpin and Lim, 2001). Mineral species was calculated as Mineral= 1.89 Al +2.14 Si + 1.4 Ca + 1.43 Fe + 1.66 Mg (Zhang et al., 2003). The concentrations of Al, Si, Fe and Mg were calculated by the concentration of Ca and the composition of urban soils of Beijing: Al= 1.7Ca, Si= 7.3Ca, Fe=0.7Ca, Mg= 0.3Ca (An et al., 2016). “Others” were calculated by subtracting

OM, EC, Mineral and secondary inorganic aerosol (SIA, including SO_4^{2-}, NO_3^-, NH_4^+) concentration from total $PM_{2.5}$ concentration. The correlation of measured and reconstructed $PM_{2.5}$ mass could be seen in Fig. S6 with R^2=0.915.

2.2 Methodology

2.2.1 Positive Matrix Factorization (PMF)

To qualitatively and quantitatively identify sources of $PM_{2.5}$ and estimate the associated contributions, the USEPA PMF 5.0 model was adopted in this study. The principle and detailed information of this model could be found in Paterson et al. (1999) and the EPA 5.0 Fundamentals and User Guide. Factor contributions and profiles were derived by minimizing the objective function Q in the PMF model, which was determined as follows (Norris et al., 2014; Paatero and Tapper, 1994; Paatero et al., 2014; Paatero, 1997):

$$Q = \sum_{i=1}^{n} \sum_{j=1}^{m} \left[\frac{x_{ij} - \sum_{k=1}^{p} g_{ik} f_{kj}}{u_{ij}}\right]^2 \quad (1)$$

Data values below the MDL were substituted with MDL/2. Missing data values were substituted with median concentrations. If the concentration was less than or equal to the MDL, the uncertainty (Unc) was calculated using a fixed fraction of the MDL:

$$Unc = \frac{5}{6} MDL \quad (2)$$

If the concentration was greater than the MDL provided, the calculation was based on the following equation:

$$Unc = \sqrt{(Error\ Fraction \times concentration)^2 + (0.5 \times MDL)^2} \quad (3)$$

In total, nineteen chemical components were used in the PMF model, including OC, EC, Cl^-, SO_4^{2-}, NO_3^-, Na^+, NH_4^+, K, Ca, Ba, Cr, Mn, Fe, Cu, Ni, Zn, As, Se and Pb. To determine the optimal number of source factors, a string of effective test, in which factors number was from four to nine, was carried out. The resulting Q parameters were shown in Fig. S4. Obviously, there was a lowest Q_{Robust} value (13087)

at six factors in moving from four to nine factors. Although $Q_{expected}$ has been decreasing in the process, $Q/Q_{expected}$ shared similar variation with Q_{Robust} showing the lowest value at six factors (see Fig. S4). Bootstrapping (BS), displacement (DISP), and bootstrapping with displacement (BS-DISP) were conducted to analyze the uncertainty of the PMF model at six factors. The results were stable with all factors mapped in BS in 100% and no swaps with DISP and all BS-DISP runs, indicating a convincing source apportionment result (see Table S2).

2.2.2 Footprint analysis model

The footprint model developed by Peking University was used to simulate the potential source region of air pollution. The footprint is a transfer function in a diffusion problem linking the source and the measurement result at a point (receptor) (Pasquill and Smith, 1977). That is,

$$c(r) = \int_R Q(r + r')f(r, r')dr' \quad (4)$$

where c is the measured concentration at spatial location r, Q is the source strength with spatial location $(r + r')$, f is the footprint or the transfer function and *R* is the integration domain. The footprint links point measurements (receptors) in the atmosphere to upstream forcings, in which turbulent dispersion plays a central role. The Lagrangian stochastic (LS) particle models was used to calculate the footprint function (Cai et al., 2007; Leclerc and Thurtell 1990; Kurbanmuradov and Sabelfeld 2000).

The meteorological data used to drive footprint model was provided by the Weather Research and Forecasting model (WRF-ARWv3.6.1) (http://www.wrf-model.org/), initialized using the Final Analysis (FNL) data from the United States National Centers for Environmental Prediction (NCEP). Two nested domains were used in this study with horizontal resolutions of 15 and 5 km, and 28 vertical levels. The simulation period was from November 1 to December 31, 2016, with a 12 h spin-up time before the start for each 48 h simulation. The domain of the footprint model is the same as the domain 2 in WRF which covers the North China Plain (500×600km), and the horizontal resolution is 2.5 × 2.5 km. Every hour,

5000 particles were released 10 m above the ground at the center of Beijing, and then each particle was tracked backward in time for 48 hours. The residence time of all particles in 0-100 m above the ground were recorded to obtain the footprint. This model has undergone rigorous theoretical discussion and verification and more detailed principle and calculation methods of the model can be found in Cai et al. (2007).

2.2.3 The Nested Air Quality Prediction Model System (NAQPMS)

In this study, the NAQPMS model was applied to analyze the contribution of local emissions and regional transport to $PM_{2.5}$ in winter in Beijing. NAQPMS is a 3-D Eulerian chemical transport model with terrain-following coordinates, developed by the Institute of Atmospheric Physics, Chinese Academy of Sciences (IAP/CAS) and has been validated by the Ministry of Environmental Protection of China (CMEP, 2013). The main modules in the model include horizontal and vertical advection and diffusion, dry and wet deposition, and gaseous, aqueous, aerosol and heterogeneous chemistry (Li et al., 2007; Li et al., 2017c). A more detailed description of the model can be found in Li et al. (2008; 2014; 2016; 2017c).

Three nested model domains were used in this study. The coarsest domain (D1) covered most of China and East Asia with a 27 km resolution. The second domain (D2) included most anthropogenic emissions within the North China Plain with a 9 km resolution. The innermost domain (D3) covered the Beijing-Tianjin-Hebei region at a 3 km resolution. The first level of model above the surface is 30 m in height, and the average vertical layer spacing between 30 m and 1 km is around 100 m. The MIX (http://www.meicmodel.org/dataset-mix.html) anthropogenic emission inventory was used (Li et al., 2017d), with the original resolution of 0.25 °(about 25 km at middle latitudes) and the year of 2010. The NAQPMS meteorological fields was provided by the Weather Research and Forecasting model (WRF-ARWv3.6.1) (http://www.wrf-model.org/) driven by the National Centers for Environmental Prediction (NCEP) Final Analysis (FNL) data. The simulation was conducted from November 10 to December 15, 2016.

2.2.4 The combination of multiple models

The footprint model was used to provide the direction of source regions while the NAQPMS model was run to calculate the contribution of local emission and regional transport. To verify the consistency between the two models, the footprint with a time resolution of 6 hours was divided into four types (local, south, north and east) according to the direction of potential source regions, and average local contributions of different types obtained from NAQPMS were calculated (See Table S3). Based on the input data availability, the footprint simulation was performed from 1-31 December while the NAQPMS model analysis was carried out from 10th of November to 15th of December. Therefore, we use the data from December 1st to 15th for the consistency test of NAQPMS and the footprint model. A typical example of different types of footprint can be seen in Fig. S5. The average local contribution estimated by NAQPMS was highest for the local footprint (85%) and lower for south (68%), north (63%) and east footprints (66%). The results of the two models correlated well with each other.

Based on online measurement of $PM_{2.5}$ species including specific source tracers, the receptor model (PMF) could be used to obtain precise source apportionment result but with no information upon regional transport. Therefore, the footprint and NAQPMS model were simultaneously conducted and combined with the PMF model to link the source type and contribution to $PM_{2.5}$ in Beijing by receptor models with different source regions.

3. Results and discussion

3.1 Mass concentration and chemical composition of $PM_{2.5}$

Temporal variation of chemical composition of $PM_{2.5}$ during the field campaign was shown in Fig. 1. The statistical summary of identified species of $PM_{2.5}$ in the entire sampling period was summarized in Table S1. Figure 1 shows that SIA and OM were the predominant $PM_{2.5}$ components in winter in Beijing, accounting for 57% and 24% of total $PM_{2.5}$ mass, respectively. The average concentration of OC was 20.

8±17.0 μg m^{-3}, and the average concentration of EC was 5.6 ±4.4 μg m^{-3}. The OC/EC ratio is often used to indicate the contribution of primary emission sources and secondary organic aerosols (SOA) (Lim et al., 2002; Zheng et al., 2014). In this study, the OC/EC ratio ranged from 1.36 to 7.92 with an average ratio of 3.91±0.91, which was lower than that in the winter of Beijing in 2013 (5.73 ±2.47) (Yan et al. 2015). SO_4^{2-} is the predominant ion in SIA with an average concentration of 23.5±20.8 μg m^{-3}, which was similar with that of NO_3^- (22.0±23.3 μg m^{-3}). The concentration of elemental components ranked from high to low as K> Fe> Ca> Zn> Pb> Mn> Ba> Cu> As> Cr> Se> Ni, with K contributing 2% to $PM_{2.5}$. In general, the large contribution of SIA, OM as well as the high OC/EC ratio indicated the importance of secondary formation in winter in Beijing (Sun et al., 2016b), while the high concentration of species like SO_4^{2-} and K suggested a significant contribution of combustion sources including coal combustion and biomass burning to $PM_{2.5}$ (Achad et al., 2018; Chen et al., 2017; Li et al., 2017b).

Figure 2 shows the large differences in chemical composition of $PM_{2.5}$ concentration between non-haze and haze episodes. The average concentration of $PM_{2.5}$ and identified species in different haze and non-haze periods were summarized in Table S4. Under low $PM_{2.5}$ concentration (< 50 μg m^{-3}), SO_4^{2-} was one of the major components of $PM_{2.5}$ with the contribution of around 24%. When $PM_{2.5}$ was from 50~150 μg m^{-3}, OM was the dominant composition (about 38%). When $PM_{2.5}$ was greater than 150 μg m^{-3}, the contribution of SIA increased with the concentration level (up to 55%). The contribution of mineral components decreased from 8% to 2% when $PM_{2.5}$ concentration increased from below 50 μg m^{-3} to over 250 μg m^{-3}. The proportion of K, Pb, As and Se, which were tracers of biomass burning and coal combustion (Achad et al., 2018; Chen et al., 2017; Vejahati et al., 2010), increased with $PM_{2.5}$ concentration. While the contribution of Ca, Ba, Fe, tracers of dust source (Amato et al., 2013; Shen et al., 2016), decreased with $PM_{2.5}$ concentration. Taken together, all these variations of source specific $PM_{2.5}$ compositions suggested more significant influence of combustion sources to $PM_{2.5}$ in haze episodes and relatively higher contribution of dust source in non-haze periods.

3.2 Source apportionment during haze and non-haze periods

To conduct high-time resolution source apportionment in Beijing, a PMF model was applied to 1-h online measurement data. The six-factor solution gave the best performance. The factor profile for each factor is shown in Fig. S7. Contribution of different factors to $PM_{2.5}$ were estimated after considering major sources in Beijing, the similarity of the PMF source profiles with relevant source emission profiles, and distinctively different marker species for different sources. Factor 1 was heavily weighted by secondary inorganic ions (SO_4^{2-}, NO_3^- and NH_4^+) and moderately weighted by OC, which was typical of the secondary source profiles (Gao et al., 2016; Peng et al., 2016; Shi et al., 2017). Factor 2 was highly loaded on metal species including Mn, Fe, Cu and Zn, which were mostly used as indicators for industrial sources (Hu et al., 2015; Li et al., 2017e; Pan et al., 2015; Yu et al., 2013). Factor 3 presented high loading of Ca, Ba, and Fe, and the two crustal elements were mainly emitted from dust sources (Amato et al., 2013; Shen et al., 2016). Factor 4 was mostly loaded by EC, OC and moderately loaded by Cu and Zn, which were mainly emitted from lubricant additive of vehicles (Kim et al., 2003; Tao et al., 2014) and wear of brake and tyre (Pant and Harrison, 2013). High loading of As, Se and moderate loading of OC, EC were observed in Factor 5, indicating a typical source profile of coal combustion (Vejahati et al., 2010). Factor 6 was characterized by high loading of K, SO_4^{2-} and OC, which were identified as indicators of biomass burning (Duan et al., 2004). In previous studies, cooking source could be one of the important sources of $PM_{2.5}$, contributing to about 10% on average in East Asia (Chafe et al., 2014; Sun et al., 2013), but in this study cooking source was not identified by PMF due to the lack of organic tracers. The relationships between the tracers of identified sources and sources mass concentrations were shown in Fig. S8.

The source apportionment result of PMF in winter in Beijing was shown in Fig. 3. During the campaign, the source contribution in Beijing ranked as secondary source (44%) > traffic source (18%) > coal combustion (16%) > biomass burning (9%) > industrial source (8%) > dust (5%). The high contribution of secondary sources in winter was similar to previous studies (Gao et al., 2016; Peng et al.,

2016; Zhang et al., 2013), which might be attributed to regional transport and heterogeneous reactions (Ma et al., 2017).

Considering data integrity and representativeness, four typical pollution episodes (EP1-4) and two non-haze periods (NH1 and NH2) were selected. The average $PM_{2.5}$ concentrations in four haze episodes were all above 97 μg m^{-3} (see Table S4). EP1 (Nov. 14-19) and EP2 (Nov. 24-27) represented the pollution episodes in November, and EP3 (Dec. 1-5) and EP4 (Dec. 16-21) were two severe pollution processes in December. The four pollution episodes were characterized by low wind speed around 2 m s^{-1} and high relative humidity (RH) compared to non-haze periods (see in Table 1). The chemical composition and sources of the four pollution episodes varied from each other, but relatively high contribution of secondary source was observed in all episodes (32-57%), and the contribution increased with $PM_{2.5}$ concentration (see Fig. 2). EP4 was characterized by the highest contribution of secondary source (57%). The contribution of coal combustion and industrial source in EP1 was the most significant compared with other episodes, which were 22% and 17% respectively. The traffic source contribution in EP2 and EP3 were higher than other pollution episodes, accounting for about 22%. The source contribution in non-haze periods was significantly different from that in pollution episodes. The contribution of secondary source in the two non-haze periods, NH1 (Nov. 22-23) and NH2 (Dec. 13-15), decreased to 18% and 25%, while traffic and dust source contribution to $PM_{2.5}$ increased to about 30% and 10%, which could be influenced by local emission and regional transport from northern areas to Beijing.

Generally, secondary source was predominant (~50%) to $PM_{2.5}$ in pollution episodes, while traffic source (~30%) became more important in non-haze periods. However, source contribution of $PM_{2.5}$ could vary from episode to episode. EP1 was more influenced by primary sources while EP4 was characterized by high secondary source contribution (57%).

3.3 Evolution of different types of haze episodes

The high-time resolution source apportionment result by PMF was combined with the NAQPMS

and footprint modelling outcomes to investigate the variation of source types and contributions with source regions in different haze episodes in Beijing. EP1 and EP4, with the longest duration and significantly different source compositions, were selected as two case episodes for further analysis.

330

3.3.1 A haze episode dominated by local emission

Figure 4 shows the variation of sources and local contribution and Fig. 5 shows the footprint regions and daily source apportionment results by PMF in EP1. The spatial mass concentrations of $PM_{2.5}$, wind speed and wind direction during EP1 by NAQPMS could be found in Fig. S9. It can be seen that EP1 was 335 characterized with high local contribution (69%-89%) and primary source contribution to $PM_{2.5}$. On November 14, the footprint located in the northeastern part to Beijing (mainly Inner Mongolia) with low $PM_{2.5}$ concentration while the contribution of dust source was significant (52%). On November 16 when the formation stage of EP1 started, the footprint concentrated in local areas of Beijing and the local contribution by NAQPMS (82%) increased simultaneously. The daily average source contribution ranked 340 as traffic source (29%) > coal combustion (28%) > industrial source (15%) > dust and secondary source (12%) > biomass burning (6%). The contribution of primary sources especially for traffic source increased when footprints were primarily located in local area.

The relationship between source apportionment and the footprint model results could also be found in the daily variation of November 17 (see Fig. 5). From 01:00 to 12:00 of the day, the footprint remained 345 in local areas while primary sources were predominant. However, with the footprint changed to southwestern areas to Beijing from 13:00 to 18:00, the contribution of secondary sources increased significantly to 42%. After the footprint changed back to local type from 19:00 to 24:00, the secondary source contribution decreased to previous level (19%).

350 **3.3.2 A haze episode dominated by regional transport**

Figure 6 shows the variation of sources and Fig. 7 shows the footprint regions and daily source

apportionment results by PMF in EP4. Different from EP1, the footprint in EP4 was mostly located in the southwestern area to Beijing, where there were heavy polluted cities including Baoding and Shijiazhuang (see Fig. 7). The daily local and regional contribution by NAQPMS of this episode was not provided due to lack of data. From the formation stage (December 16 -17) to the peak (December 20) of EP4, the contribution of secondary sources increased from 34% to 58%, while the contribution of coal combustion and biomass burning were also significant among primary sources (see Fig. 6). Figure 7 shows that the footprint on December 17 was more concentrated in local and eastern areas to Beijing, while it gradually moved to southwestern areas along with the increase of $PM_{2.5}$ concentration and the secondary source contribution.

The above results confirmed that high-time resolution source apportionment result could be integrated with footprint and NAQPMS model to identify the rapid evolution of different episodes - EP1 was an episode mainly caused by local emission from transportation and coal combustion while EP4 was typical for regional transport from southwestern areas to Beijing with increasing contributions of secondary sources.

3.4 Relationship of $PM_{2.5}$ sources by PMF with regional transport estimated by NAQPMS

3.4.1 Sources dominated by local emission and regional transport

Receptor models which are used for source apportionment have the limitation that it could not quantify the local or regional transport contribution. Therefore, the receptor model was combined with the chemical transport model NAQPMS to investigate the correlation of source contribution with local/regional transport. As shown in Sect. 3.2, secondary and combustion sources were predominant in haze episodes in Beijing. To better control those major sources in winter, it is essential to determine correlation of source contribution with the contribution of local emission or regional transport. Figure 8 shows the correlations of relative contribution of secondary sources, coal combustion and biomass burning sources by PMF with local contribution by NAQPMS during the sampling period. The results

showed that for $PM_{2.5}$ in Beijing, secondary source contribution decreased when local emission was more significant ($p<0.05$, $r=0.4$) while coal combustion, as a primary combustion source, showed an increasing trend along with local contribution estimated by NAQPMS ($p<0.05$, $r=0.3$). Comparing with Fig. 8 (b) and (c), the two primary combustion sources showed opposite relationship with local contribution, indicating that the pollutants from biomass burning were mainly transported from surrounding areas outside of Beijing while those from coal combustion were more influenced by local emission. According to previous studies, biomass burning was an important source in provinces around Beijing including Shandong, Hebei and Inner Mongolia (Khuzestani et al., 2018; Sun et al., 2016a; Zhang et al., 2010; Zhao et al., 2012; Zong et al., 2016). The surrounding provinces and cities of Beijing are shown in Fig. S10. The results suggested that local-emitted coal combustion contributed significantly to $PM_{2.5}$ in Beijing in winter 2016 and the strict control strategies for coal combustion were essential to improve air quality in Beijing. In the meantime, more control of biomass burning and precursors of secondary source in surrounding areas are also needed to mitigate air pollution in Beijing.

3.4.2 Sources dominated in different potential source regions

The combination of PMF result with footprint model was used to further identify specific source type and contribution in different source regions. As mentioned in Sect. 2.2.4, the footprint with the time resolution of 6 hours was divided into four types (local, south, north and east) according to the direction of potential source regions. The typical examples of different types of footprint were shown in Fig. S5. The local footprint referred to the cases with source region located within Beijing. The south footprint mainly covered southwest areas in Hebei province including Baoding, Shijiazhuang and Xingtai. The north footprint included Zhangjiakou and Inner Mongolia. The east footprint covered the north part of Hebei such as Tangshan and Qinhuangdao and the south part of Liaoning province. The local footprint was predominant in winter in Beijing (N=79) with the contribution of 38%, followed by north and south footprint (N=51, 45 respectively). The amount of east footprint was the lowest in

winter. The average value and box chart of source contribution in four types of footprint during the whole sampling period were shown in Fig. 9. It could be seen that local footprint was characterized by traffic (23%) and coal combustion source (25%), while the contribution of secondary source (26%) was the lowest among the four types. On the contrary, secondary source was predominant in south footprint cases with the contribution of 53%, while the contribution of traffic source decreased to 15%. The results corresponded well with the analysis of two typical episodes in Sect. 3.3. North footprint was characterized by the highest contribution of dust source (11%), which could be influenced by dust transported from Inner Mongolia (Hoffmann et al., 2008; Park et al., 2014). East footprint, which mainly covered heavy industrial areas such as Tangshan and Shenyang, showed higher contribution of industrial sources (10%) and coal combustion sources (18%). Figure 9 (b) shows that the variation of source contribution was the smallest in local footprint, indicating a relatively stable local emission of Beijing, while the source contribution varied more significantly with east footprint.

The results of PMF and footprint model showed that source contribution in winter in Beijing was influenced by the potential source regions, and the predominant source could change specifically for different footprint type, which might suggest that source apportionment and footprint analysis need to be combined to better control specific sources from different source regions.

3.5 Future prospect

In this study, the high-time resolution online measurement was conducted by Xact, IGAC and the Sunset OCEC analyzer, which could measure inorganic species including water-soluble ions, elemental components, OC and EC. As a result, most of the tracers selected for PMF source apportionment were inorganic species. In previous studies based on online measurement, organic tracers are also not commonly used due to current technical difficulty in carrying out online and quantitative measurements of organic species with high-time resolution (Gao et al., 2016; Li et al., 2017e; Peng et al., 2016). However, some organic tracers are believed to be more specific for certain sources, such as levoglucosan for biomass

burning, hopane and sterane for traffic source, and cholesterol for cooking source (Fraser et al., 2000; Yin et al., 2010; Zhao et al., 2015). Therefore, future online measurement of organic species could be conducted, which will be very helpful in identifying sources. Besides, vertical measurement of $PM_{2.5}$ is important for better understanding of sources and regional transport of $PM_{2.5}$ in Beijing. Li et al. (2017) found that the height of regional transport ranged from 200 to 700 m above ground level using the NAQPMS model. In the future, the integration of ambient measurement with the air quality model should be considered in a vertical level as well.

4. Summary

High-time resolution online measurements of $PM_{2.5}$ were conducted during the APHH winter campaign in Beijing. Considering the limitation of receptor models which could not identify and quantify regional transport, the receptor model PMF was combined with multiple models including NAQPMS and footprint model to analyze the specific sources from different source regions during haze episodes in Beijing. The source apportionment results by PMF during our sampling period showed that secondary source was predominant (~50%) to $PM_{2.5}$ in pollution episodes, while traffic source (~30%) became more important in non-haze periods. Source contribution of $PM_{2.5}$ could vary from episode to episode.

The multiple models were combined to analyze the evolution of two typical pollution episodes in Beijing. The high-time resolution results indicated that source contribution could vary rapidly and significantly with source regions within different types of haze episodes. EP1, with local concentrated footprint and high local emission, was characterized by coal combustion and traffic source while EP4 with more southwestern footprint was typical for high secondary source contribution. The relationship of $PM_{2.5}$ sources by PMF with regional transport during the whole sampling period was further investigated. As the predominant sources of $PM_{2.5}$ in Beijing, secondary and biomass burning source were more influenced by regional transport while coal combustion source increased with local contribution. The source regions of $PM_{2.5}$ in Beijing were classified into four types and source contribution varied

significantly with potential source regions, with traffic source dominated in local footprint, secondary source dominated in south footprint, dust and industrial source increased in north and east footprint, respectively. The results suggested that source contribution of $PM_{2.5}$ in winter, Beijing could change significantly along with the contribution and direction of regional transport. Therefore, the combined use of receptor model, meteorological model and chemical transport model was important to identify specific sources from different source regions.

Acknowledgements

This study was supported by funding from the National Natural Science Foundation of China (41571130033, 41430646, 41571130035, 91744203 and 41571130034). Z.S. and R.M.H. acknowledge support from UK Natural Environment Research Council (NE/N006992/1 and NE/R005281/1). The authors gratefully thank for the assistance of Jinting Yu in Peking University for maintaining the online instruments in this work.

Reference

Achad, M., Caumo, S., de Castro Vasconcellos, P., Bajano, H., Gómez, D., and Smichowski, P.: Chemical markers of biomass burning: Determination of levoglucosan, and potassium in size-classified atmospheric aerosols collected in Buenos Aires, Argentina by different analytical techniques, Microchem. J., 139, 181-187, 2018.

Amato, F., Schaap, M., van der Gon, H. A. D., Pandolfi, M., Alastuey, A., Keuken, M., and Querol, X.: Short-term variability of mineral dust, metals and carbon emission from road dust resuspension, Atmos. Environ., 74, 134-140, 2013.

An, Y. L., Huang, Y., Liu, Q. J., Sun, C., Deng, K. W., Li, D., and Huang, D.: The distribution of surface soil elements and the pollution assessment of heavy metal elements in Beijing. Geological Bulletin of China, 35(12):2111-2120, 2016 (in Chinese).

Bauer, J. J., Xiao-Ying, Y., Robert, C., Nels, L., and Carl, B.: Characterization of the sunset semi-continuous carbon aerosol analyzer, Air Repair, 59, 826-833, 2009.

Burr, M. J., and Zhang, Y.: Source apportionment of fine particulate matter over the Eastern US Part I: source sensitivity simulations using CMAQ with the Brute Force method, Atmos. Pollut. Res., 2, 300-317, 2011.

Cai, X., and Leclerc, M. Y.: Forward-in-time and backward-in-time dispersion in the convective boundary layer: the concentration footprint, Boundary Layer Meteorol., 123, 201-218, 2007.

Chafe, Z. A., Michael, B., Zbigniew, K., Rita, V. D., Sumi, M., Shilpa, R., Keywan, R., Frank, D., and Smith, K. R.: Household cooking with solid fuels contributes to ambient $PM_{2.5}$ air pollution and the burden of disease, Environ. Health Perspect., 122, 1314-1320, 2014.

Chen, S., Guo, Z., Guo, Z., Guo, Q., Zhang, Y., Zhu, B., and Zhang, H.: Sulfur isotopic fractionation and its implication: Sulfate formation in $PM_{2.5}$ and coal combustion under different conditions, Atmos. Res., 194, 142-149, 2017.

Cooper, J. A., and Watson Jr, J. G.: Receptor oriented methods of air particulate source apportionment, J. Air Pollut. Control Assoc., 30, 1116-1125, 1980.

China Ministry of Environmental Protection, 2013. Technical Guidelines for Source Apportionment of Atmospheric Particulate Matter (For Trial Implementation) (in Chinese).

Duan, F., Liu, X., Yu, T., and Cachier, H.: Identification and estimate of biomass burning contribution to the urban aerosol organic carbon concentrations in Beijing, Atmos. Environ., 38, 1275-1282, 2004.

Fraser, M. P., Lakshmanan, K.: Using Levoglucosan as a molecular marker for the long-range transport of biomass combustion aerosols, Environ. Sci. Technol., 34(21), 4560-4564, 2000.

Gao, J., Peng, X., Chen, G., Xu, J., Shi, G.L., Zhang, Y.C., and Feng, Y.C.: Insights into the chemical characterization and sources of $PM_{2.5}$ in Beijing at a 1-h time resolution, Sci. Total Environ., 542, 162-171, 2016.

Han, L., Cheng, S., Zhuang, G., Ning, H., Wang, H., Wei, W., and Zhao, X.: The changes and long-range transport of $PM_{2.5}$ in Beijing in the past decade, Atmos. Environ., 110, 186-195, 2015.

Han, X., and Zhang, M.G.: Assessment of the regional source contributions to $PM_{2.5}$ mass concentration in Beijing, Atmos. Oceanic Sci. Lett., 11, 143-149, 2018.

Hoffmann, C., Funk, R., Sommer, M., and Li, Y.: Temporal variations in PM_{10} and particle size distribution during Asian dust storms in Inner Mongolia, Atmos. Environ., 42, 8422-8431, 2008.

Hu, Y., Lin, J., Zhang, S., Kong, L., Fu, H., and Chen, J.: Identification of the typical metal particles among haze, fog, and clear episodes in the Beijing atmosphere, Sci. Total Environ., 511, 369-380, 2015.

Khuzestani, R. B., Schauer, J. J., Shang, J., Cai, T., Fang, D., Wei, Y., Zhang, L., and Zhang, Y.: Source apportionments of $PM_{2.5}$ organic carbon during the elevated pollution episodes in the Ordos region, Inner Mongolia, China, Environ. Sci. Pollut. Res., 25, 13159-13172, 2018.

Kim, E., Hopke, P. K., and Edgerton, E. S.: Source identification of Atlanta aerosol by positive matrix factorization, J. Air Waste Manage, 53, 731-739, 2003.

Kotchenruther, R. A.: Source apportionment of $PM_{2.5}$ at multiple Northwest U.S. sites: Assessing regional winter wood smoke impacts from residential wood combustion, Atmos. Environ., 142, 210-219, 2016.

Kurbanmuradov, O., and Sabelfeld, K.: Lagrangian stochastic models for turbulent dispersion in the atmospheric boundary layer, Boundary Layer Meteorol., 97, 191-218, 2000.

Kwok, R. H., Napelenok, S., and Baker, K.: Implementation and evaluation of $PM_{2.5}$ source contribution analysis in a photochemical model, Atmos. Environ., 80, 398-407, 2013.

Leclerc, M., and Thurtell, G.: Footprint prediction of scalar fluxes using a Markovian analysis, Boundary Layer Meteorol., 52, 247-258, 1990.

Li, D., Liu, J., Zhang, J., Gui, H., Du, P., Yu, T., Wang, J., Lu, Y., Liu, W., and Cheng, Y.: Identification of long-range transport

pathways and potential sources of $PM_{2.5}$ and PM_{10} in Beijing from 2014 to 2015, J. Environ. Sci., 56, 214-229, 2017a.

Li, H., Zhang, Q., Zhang, Q., Chen, C., Wang, L., Wei, Z., Zhou, S., Parworth, C., Zheng, B., and Canonaco, F.: Wintertime aerosol chemistry and haze evolution in an extremely polluted city of the North China Plain: significant contribution from coal and biomass combustion, Atmos. Chem. Phys., 17, 4751-4768, 2017b.

Li, J., Wang, Z., Akimoto, H., Gao, C., Pochanart, P., and Wang, X.: Modeling study of ozone seasonal cycle in lower troposphere over east Asia, J. Geophys. Res-Atoms., 112, 2007.

Li, J., Wang, Z., Akimoto, H., Yamaji, K., Takigawa, M., Pochanart, P., Liu, Y., Tanimoto, H., and Kanaya, Y.: Near-ground ozone source attributions and outflow in central eastern China during MTX2006, Atmos. Chem. Phys., 8, 7335-7351, 2008.

Li, J., Yang, W., Wang, Z., Chen, H., Hu, B., Li, J., Sun, Y., and Huang, Y.: A modeling study of source-receptor relationships in atmospheric particulate matter over Northeast Asia, Atmos. Environ., 91, 40-51, 2014.

Li, J., Yang, W., Wang, Z., Chen, H., Hu, B., Li, J., Sun, Y., Fu, P., and Zhang, Y.: Modeling study of surface ozone source-receptor relationships in East Asia, Atmos. Res., 167, 77-88, 2016.

Li, J., Du, H., Wang, Z., Sun, Y., Yang, W., Li, J., Tang, X., and Fu, P.: Rapid formation of a severe regional winter haze episode over a mega-city cluster on the North China Plain, Environ. Pollut., 223, 605-615, 2017c.

Li, M., Zhang, Q., Kurokawa, J.-i., Woo, J.-H., He, K., Lu, Z., Ohara, T., Song, Y., Streets, D. G., and Carmichael, G. R.: MIX: a mosaic Asian anthropogenic emission inventory under the international collaboration framework of the MICS-Asia and HTAP, Atmospheric Chemistry and Physics, 17, 2017d.

Li, Y., Chang, M., Ding, S., Wang, S., Ni, D., and Hu, H.: Monitoring and source apportionment of trace elements in $PM_{2.5}$: Implications for local air quality management, J. Environ. Manage., 196, 16-25, 2017e.

Lim, H.J., and Turpin, B. J.: Origins of primary and secondary organic aerosol in Atlanta: Results of time-resolved measurements during the Atlanta supersite experiment, Environ. Sci. Technol., 36, 4489-4496, 2002.

Liu, Y., Yan, C., and Zheng, M.: Source apportionment of black carbon during winter in Beijing, Sci. Total Environ., 618, 531-541, 2018.

Lv, B., Zhang, B., and Bai, Y.: A systematic analysis of $PM_{2.5}$ in Beijing and its sources from 2000 to 2012, Atmos. Environ., 124, 98-108, 2016.

Ma, Q., Wu, Y., Zhang, D., Wang, X., Xia, Y., Liu, X., Tian, P., Han, Z., Xia, X., and Wang, Y.: Roles of regional transport and heterogeneous reactions in the $PM_{2.5}$ increase during winter haze episodes in Beijing, Sci. Total Environ., 599, 246-253, 2017.

Norris, G., Duvall, R., Brown, S., and Bai, S.: EPA Positive Matrix Factorization (PMF) 5.0 Fundamentals and User Guide, 2014.

Paatero, P.: Least squares formulation of robust non-negative factor analysis, Chemometr. Intell. Lab., 37, 23-35, 1997.

Paatero, P., and Tapper, U.: Positive matrix factorization: A non-negative factor model with optimal utilization of error estimates of data values, Environmetrics, 5, 111-126, 2010.

Paatero, P., Eberly, S., Brown, S. G., and Norris, G. A.: Methods for estimating uncertainty in factor analytic solutions, Atmos. Meas. Tech.,7,3(2014-03-27), 6, 7593-7631, 2014.

Pan, Y., Tian, S., Li, X., Sun, Y., Li, Y., Wentworth, G. R., and Wang, Y.: Trace elements in particulate matter from metropolitan regions of Northern China: Sources, concentrations and size distributions, Sci. Total Environ., 537, 9-22, 2015.

Pant, P., and Harrison, R. M.: Estimation of the contribution of road traffic emissions to particulate matter concentrations from

field measurements: a review, Atmos. Environ., 77, 78-97, 2013.

Park, S.U., and Park, M.-S.: Aerosol size distributions observed at Naiman in the Asian dust source region of Inner Mongolia, Atmos. Environ., 82, 17-23, 2014.

Pasquill, F., and Michael, P.: Atmospheric diffusion, Phys. Today, 30, 55, 1977.

Paterson, K. G., Sagady, J. L., Hooper, D. L., Bertman, S. B., Carroll, M. A., and Shepson, P. B.: Analysis of air quality data using Positive Matrix Factorization, Environ. Sci. Technol., 33, 635-641, 1999.

Peng, X., Shi, G.L., Gao, J., Liu, J.Y., HuangFu, Y.Q., Ma, T., Wang, H.T., Zhang, Y.C., Wang, H., and Li, H.: Characteristics and sensitivity analysis of multiple-time-resolved source patterns of $PM_{2.5}$ with real time data using Multilinear Engine 2, Atmos. Environ., 139, 113-121, 2016.

Pérez, N., Pey, J., Cusack, M., Reche, C., Querol, X., Alastuey, A., and Viana, M.: Variability of particle number, black carbon, and PM_{10}, $PM_{2.5}$, and PM_1 levels and speciation: influence of road traffic emissions on urban air quality, Aerosol Sci. Technol., 44, 487-499, 2010.

Pitchford, M., Malm, W., Schichtel, B., Kumar, N., Lowenthal, D., and Hand, J.: Revised algorithm for estimating light extinction from IMPROVE particle speciation data, J. Air Waste Manage., 57, 1326-1336, 2007.

Shen, Z., Sun, J., Cao, J., Zhang, L., Zhang, Q., Lei, Y., Gao, J., Huang, R.J., Liu, S., and Huang, Y.: Chemical profiles of urban fugitive dust $PM_{2.5}$ samples in Northern Chinese cities, Sci. Total Environ., 569, 619-626, 2016.

Shi, G., Xu, J., Peng, X., Xiao, Z., Chen, K., Tian, Y., Guan, X., Feng, Y., Yu, H., and Nenes, A.: pH of aerosols in a polluted atmosphere: source contributions to highly acidic aerosol, Environ. Sci. Technol., 51, 4289-4296, 2017.

Song, Y., Zhang, Y., Xie, S., Zeng, L., Zheng, M., Salmon, L. G., Shao, M., and Slanina, S.: Source apportionment of $PM_{2.5}$ in Beijing by Positive Matrix Factorization, Atmos. Environ., 40, 1526-1537, 2006.

Sun, J., Peng, H., Chen, J., Wang, X., Wei, M., Li, W., Yang, L., Zhang, Q., Wang, W., and Mellouki, A.: An estimation of CO_2 emission via agricultural crop residue open field burning in China from 1996 to 2013, J. Cleaner Prod., 112, 2625-2631, 2016a.

Sun, Y., Chen, C., Zhang, Y., Xu, W., Zhou, L., Cheng, X., Zheng, H., Ji, D., Li, J., and Tang, X.: Rapid formation and evolution of an extreme haze episode in Northern China during winter 2015, Sci. Rep., 6, 27151, 2016b.

Sun, Y., Wang, Z., Pingqing, F. U., Jiang, Q. I., Yang, T., Jie, L. I., and Xinlei, G. E.: The impact of relative humidity on aerosol composition and evolution processes during wintertime in Beijing, China, Atmos. Environ., 77, 927-934, 2013.

Taghvaee, S., Sowlat, M. H., Mousavi, A., Hassanvand, M. S., Yunesian, M., Naddafi, K., and Sioutas, C.: Source apportionment of ambient $PM_{2.5}$ in two locations in central Tehran using the Positive Matrix Factorization (PMF) model, Sci. Total Environ., 628-629, 672, 2018.

Tao, J., Gao, J., Zhang, L., Zhang, R., Che, H., Zhang, Z., Lin, Z., Jing, J., Cao, J., and Hsu, S.C.: $PM_{2.5}$ pollution in a megacity of southwest China: source apportionment and implication, Atmos. Chem. Phys., 14, 8679-8699, 2014.

Turpin, B. J., Lim, H. J.: Species contributions to $PM_{2.5}$ mass concentrations: revisiting common assumptions for estimating organic mass. Aerosol Sci. Tech., 35(1), 602-610, 2001.

Vejahati, F., Xu, Z., and Gupta, R.: Trace elements in coal: Associations with coal and minerals and their behavior during coal utilization-A review, Fuel, 89, 904-911, 2010.

Watson, J. G., Chow, J. C., and Houck, J. E.: $PM_{2.5}$ chemical source profiles for vehicle exhaust, vegetative burning, geological material, and coal burning in Northwestern Colorado during 1995, Chemosphere, 43, 1141-1151, 2001.

Watson, J. G.: Visibility: Science and regulation, J. Air Waste Manage., 52, 628-713, 2002.

Xie, Y., Dai, H., Dong, H., Hanaoka, T., and Masui, T.: Economic impacts from $PM_{2.5}$ pollution-related health effects in China: a provincial-level analysis, Environ. Sci. Technol., 50, 4836-4843, 2016.

Yan, C., Zheng, M., Sullivan, A. P., Bosch, C., Desyaterik, Y., Andersson, A., Li, X., Guo, X., Zhou, T., and Gustafsson, Ö.: Chemical characteristics and light-absorbing property of water-soluble organic carbon in Beijing: Biomass burning contributions, Atmos. Environ., 121, 4-12, 2015.

Yang, H., Chen, J., Wen, J., Tian, H., and Liu, X.: Composition and sources of $PM_{2.5}$ around the heating periods of 2013 and 2014 in Beijing: Implications for efficient mitigation measures, Atmos. Environ., 124, 378-386, 2016.

Yang, Y., Liu, X., Qu, Y., An, J., Jiang, R., Zhang, Y., Sun, Y., Wu, Z., Zhang, F., and Xu, W.: Characteristics and formation mechanism of continuous hazes in China: a case study in autumn of 2014 in the North China Plain, Atmos. Chem. Phys, 15, 8165-8178, 2015.

Yin, J., Harrison, R. M., Chen, Q., Rutter, A., and Schauer, J. J.: Source apportionment of fine particles at urban background and rural sites in the UK atmosphere, Atmos. Environ., 44, 841-851, 2010.

Young, L. H., Li, C. H., Lin, M. Y., Hwang, B. F., Hsu, H. T., Chen, Y. C., Jung, C. R., Chen, K. C., Cheng, D. H., and Wang, V. S.: Field performance of a semi-continuous monitor for ambient $PM_{2.5}$ water-soluble inorganic ions and gases at a suburban site, Atmos. Environ., 144, 376-388, 2016.

Yu, L., Wang, G., Zhang, R., Zhang, L., Song, Y., Wu, B., Li, X., An, K., and Chu, J.: Characterization and source apportionment of $PM_{2.5}$ in an urban environment in Beijing, Aerosol Air Qual. Res, 13, 574-583, 2013.

Zhang, R., Jing, J., Tao, J., Hsu, S.C., Wang, G., Cao, J., Lee, C. S. L., Zhu, L., Chen, Z., and Zhao, Y.: Chemical characterization and source apportionment of $PM_{2.5}$ in Beijing: seasonal perspective, Atmos. Chem. Phys., 13, 7053-7074, 2013.

Zhang, X., Gong, S., Shen, Z., Mei, F., Xi, X., Liu, L., Zhou, Z., Wang, D., Wang, Y., and Cheng, Y.: Characterization of soil dust aerosol in China and its transport and distribution during 2001 ACE-Asia: 1. Network observations, J. Geophys. Res-Atmos., 108, 2003.

Zhang, Y., Dore, A., Ma, L., Liu, X., Ma, W., Cape, J., and Zhang, F.: Agricultural ammonia emissions inventory and spatial distribution in the North China Plain, Environ. Pollut., 158, 490-501, 2010.

Zhang, Y., Zheng, M., Cai, J., Yan, C., Hu, Y., Russell, A., Wang, X., Wang, S., and Zhang, Y.: Comparison and overview of $PM_{2.5}$ source apportionment methods, Chin. Sci. Bull., 60, 109-121, 2015.

Zhao, B., Wang, P., Ma, J. Z., Zhu, S., Pozzer, A., and Li, W.: A high-resolution emission inventory of primary pollutants for the Huabei region, China, Atmos. Chem. Phys., 12, 481-501, 2012.

Zhao, X., Hu, Q., Wang, X., Xiang, D., He, Q., Zhou, Z., Shen, R., Lü, S., Liu, T., and Fu, X.: Composition profiles of organic aerosols from Chinese residential cooking: case study in urban Guangzhou, south China, J. Atmos. Chem., 72, 1-18, 2015.

Zhao, X., Zhao, P., Xu, J., Meng, W., Pu, W., Dong, F., He, D., and Shi, Q.: Analysis of a winter regional haze event and its formation mechanism in the North China Plain, Atmos. Chem. Phys., 13, 5685-5696, 2013.

Zheng, M., Salmon, L. G., Schauer, J. J., Zeng, L., Kiang, C., Zhang, Y., and Cass, G. R.: Seasonal trends in $PM_{2.5}$ source contributions in Beijing, China, Atmos. Environ., 39, 3967-3976, 2005.

Zheng, M., Zhao, X., Cheng, Y., Yan, C., Shi, W., Zhang, X., Weber, R. J., Schauer, J. J., Wang, X., and Edgerton, E. S.:

Sources of primary and secondary organic aerosol and their diurnal variations, J. Hazard. Mater., 264, 536-544, 2014.
Zong, Z., Wang, X., Tian, C., Chen, Y., Qu, L., Ji, L., Zhi, G., Li, J., and Zhang, G.: Source apportionment of $PM_{2.5}$ at a regional background site in North China using PMF linked with radiocarbon analysis: insight into the contribution of biomass burning, Atmos. Chem. Phys., 16, 11249-11265, 2016.

Tables and Figure Legends

Table 1. Meteorological conditions during pollution episodes and non-haze periods.

Figure 1. Chemical composition of $PM_{2.5}$ during sampling period (red for SO_4^{2-}, blue for NO_3^-, yellow for NH_4^+, green for OM, black for EC, pink for mineral, and grey for others).

Figure 2. Variation of (a) chemical composition and (b) elemental species with $PM_{2.5}$ concentration (the white bars represent the frequency of $PM_{2.5}$ concentration).

Figure 3. Source contribution of $PM_{2.5}$ (a) in the whole sampling period and (b) in different pollution episodes and non-haze periods (yellow for dust source, green for biomass burning, pink for industrial source, red for coal combustion, black for traffic source, and blue for secondary source).

Figure 4. Variation of sources and local contribution during EP1. The above pie charts show the daily local (Beijing as BJ) and regional contribution (labeled as Others). The pie charts below show the daily source type and contribution.

Figure 5. (a) Source regions by the footprint model and (b) daily source apportionment results by PMF in EP1.

Figure 6. Source contribution in EP4. The pie charts show the daily source type and contribution.

Figure 7. (a) Source regions by the footprint model and (b) daily source apportionment results by PMF in EP4.

Figure 8. Correlations of local contribution by NAQPMS with the relative contribution by PMF of (a) secondary source, (b) coal combustion source and (c) biomass burning source.

Figure 9. (a) The average source contribution (in percentage) for each type of footprint, and (b) box chart of source contribution in four types of footprint during the whole sampling period. N in (a) represents for the number of cases. The capital letters in (b) stands for the type of footprint (L for local; S for south; N for north; E for east) and the lowercases stands for different sources (s for secondary source, c for coal combustion, t for traffic source, i for industrial source, d for dust, and b for biomass burning).

Table 1. Meteorological conditions during pollution episodes and non-haze periods.

	EP1	EP2	EP3	EP4	Non-haze	Average
Wind speed (m s^{-1})	2.24	2.26	2.36	2.04	4.17	2.48
Temperature (℃)	7.48	2.94	5.36	2.63	-2.05	3.42
Relative humidity (%)	54.5	38.2	38.8	49.4	24.1	43.5
Pressure (hPa)	1012.5	1016.5	1016.3	1016.1	1027.9	1017.4

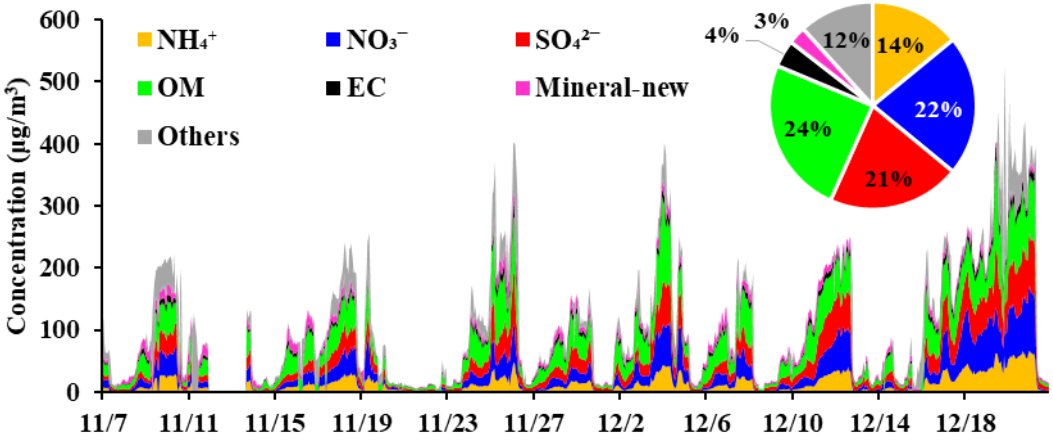

Figure 1. Chemical composition of $PM_{2.5}$ during sampling period (red for SO_4^{2-}, blue for NO_3^-, yellow for NH_4^+, green for OM, black for EC, pink for mineral, and grey for others).

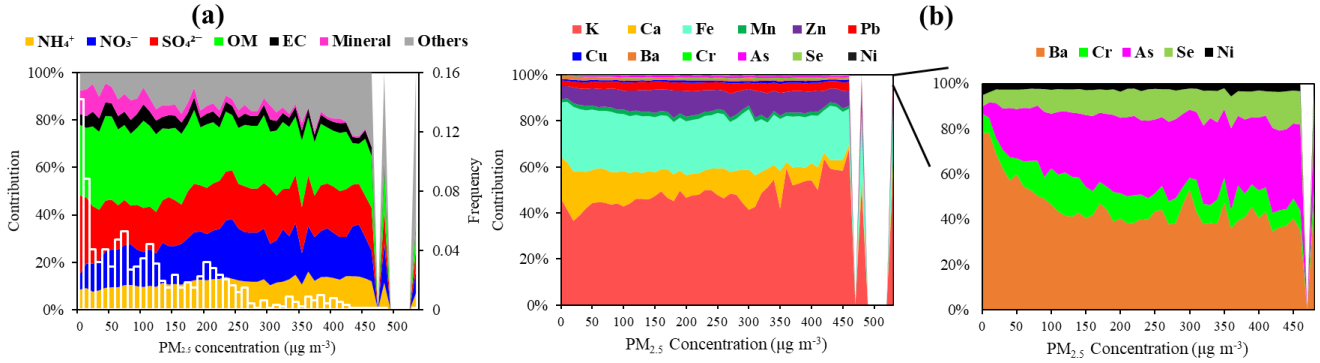

Figure 2. Variation of (a) chemical composition and (b) elemental species with $PM_{2.5}$ concentration (the white bars represent the frequency of $PM_{2.5}$ concentration).

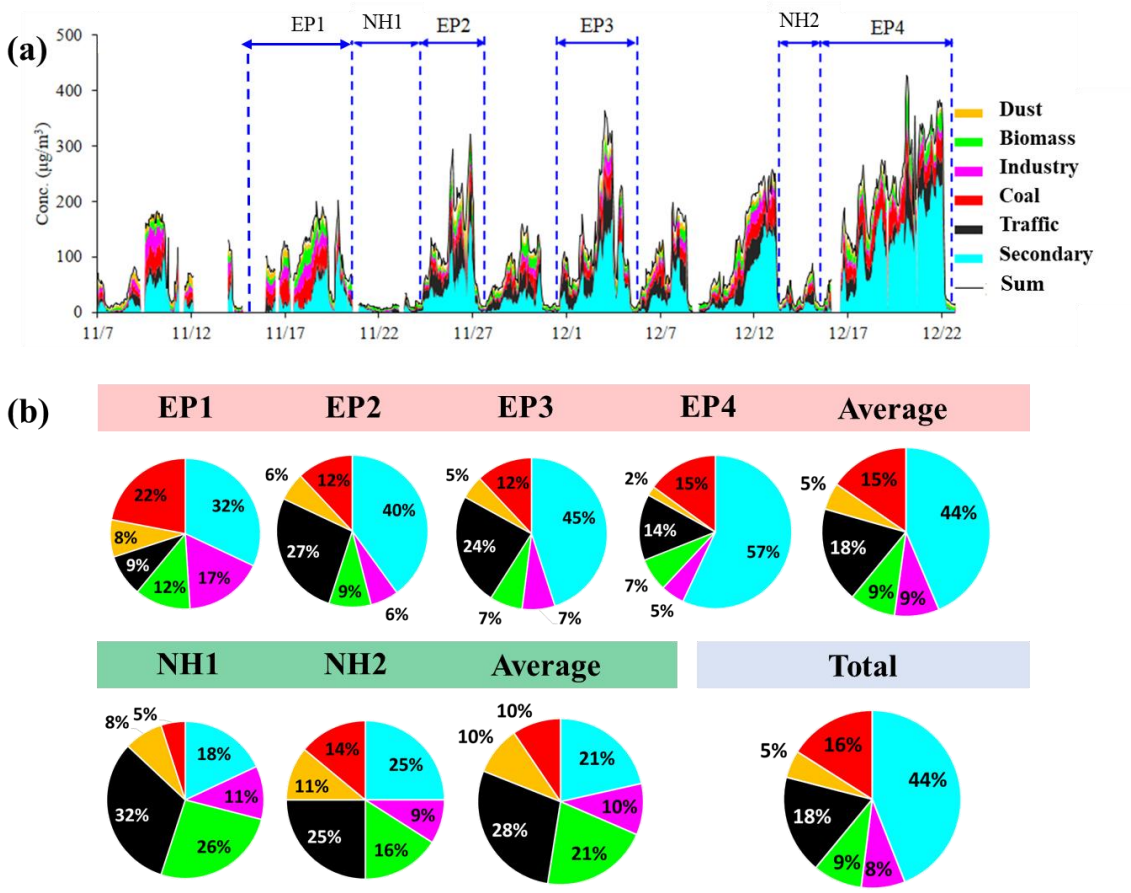

Figure 3. Source contribution of $PM_{2.5}$ (a) in the whole sampling period and (b) in different pollution episodes and non-haze periods (yellow for dust source, green for biomass burning, pink for industrial source, red for coal combustion, black for traffic source, and blue for secondary source).

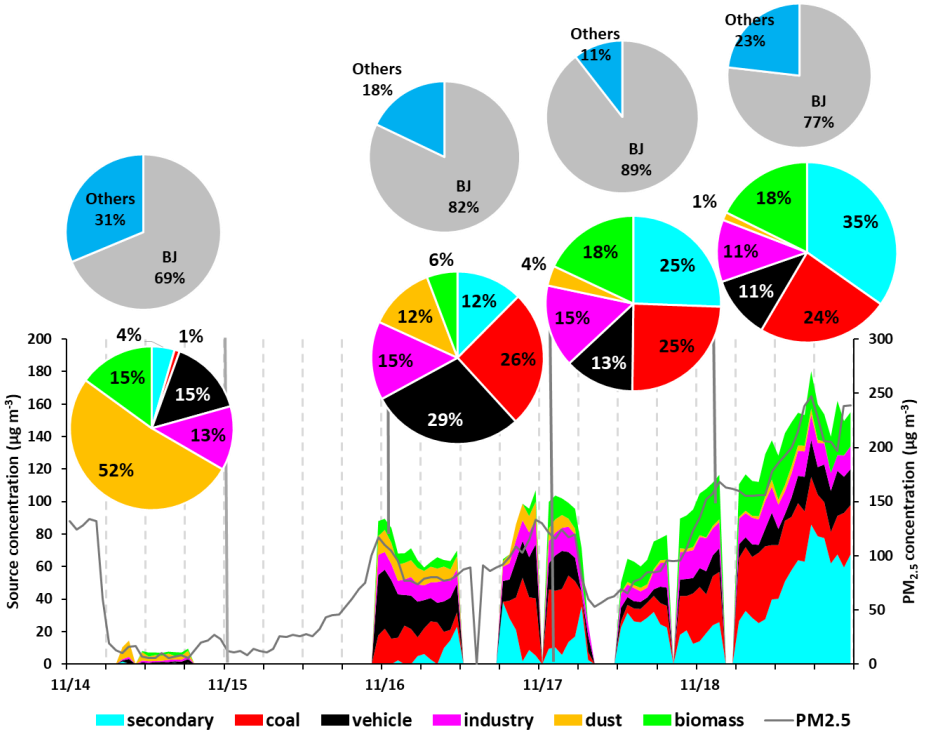

Figure 4. Variation of sources and local contribution during EP1. The above pie charts show the daily local (Beijing as BJ) and regional contribution (labeled as Others). The pie charts below show the daily source type and contribution.

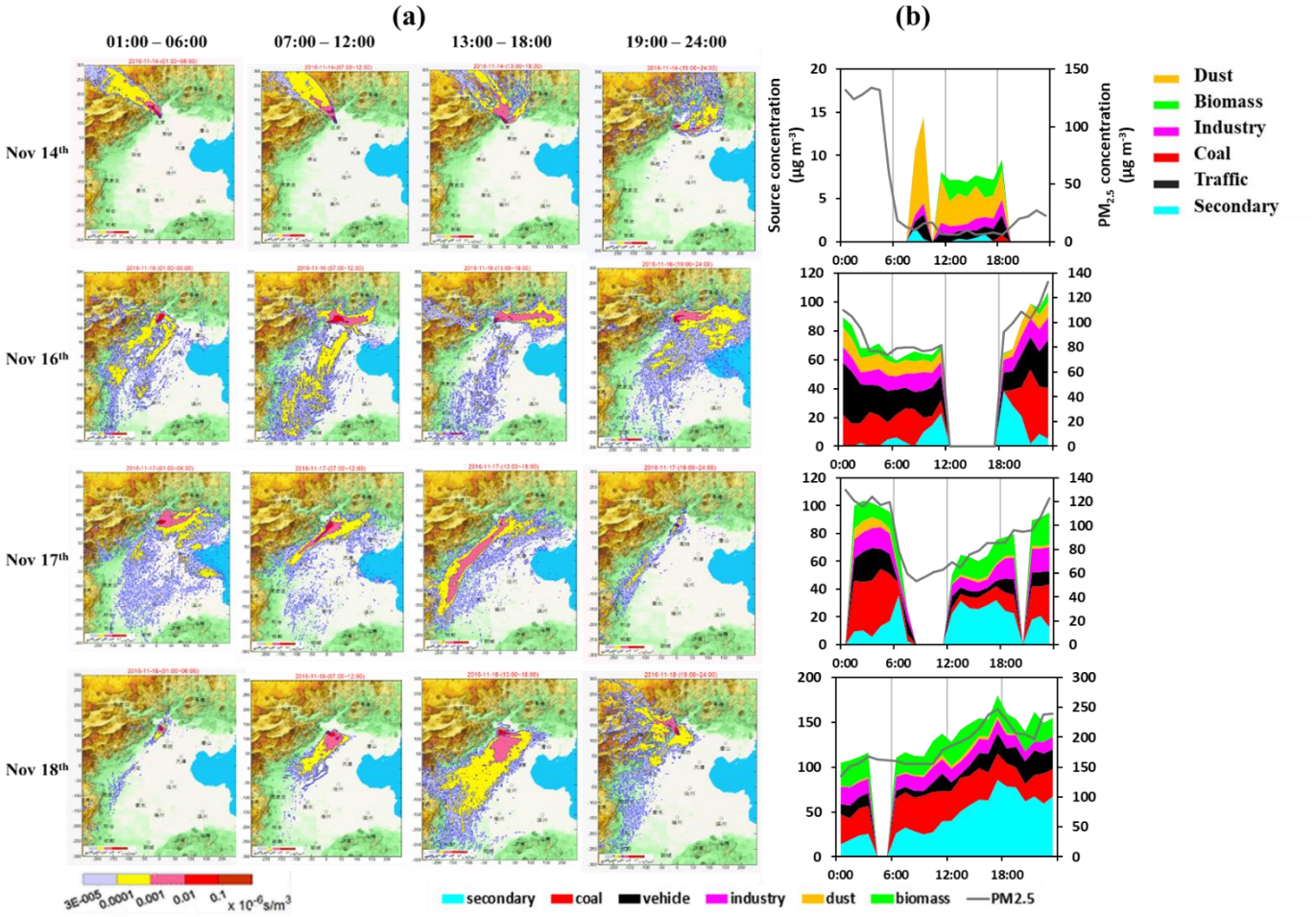

Figure 5. (a) Source regions by the footprint model and (b) daily source apportionment results by PMF in EP1.

720

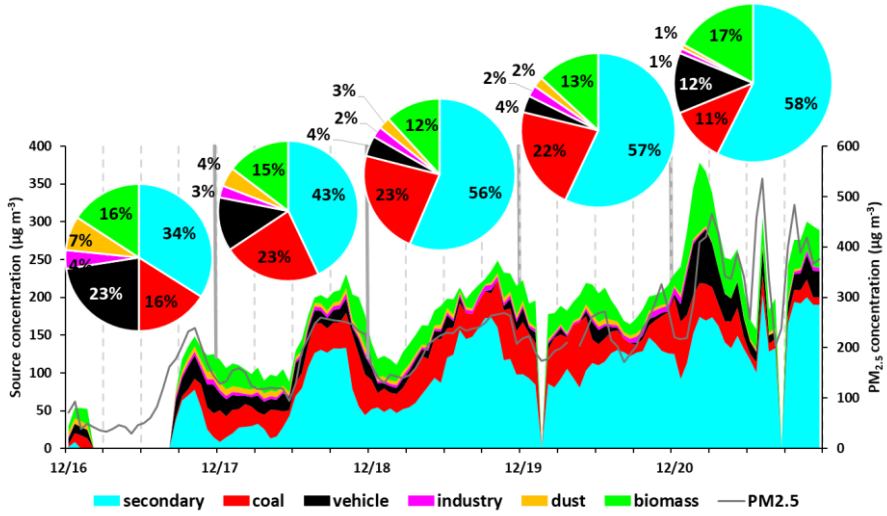

725 **Figure 6.** Source contribution in EP4. The pie charts show the daily source type and contribution.

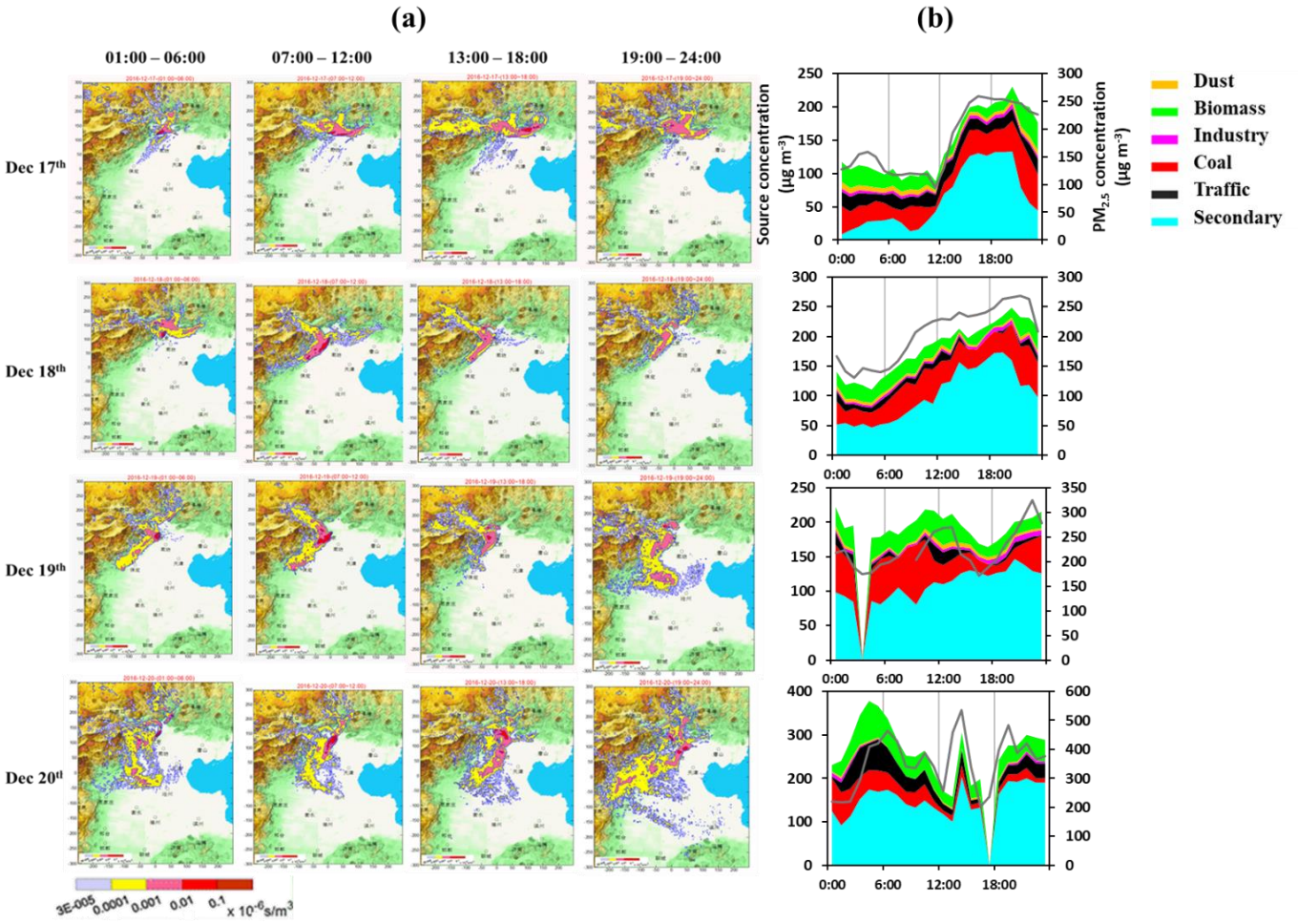

Figure 7. (a) Source regions by the footprint model and (b) daily source apportionment results by PMF in EP4.

730

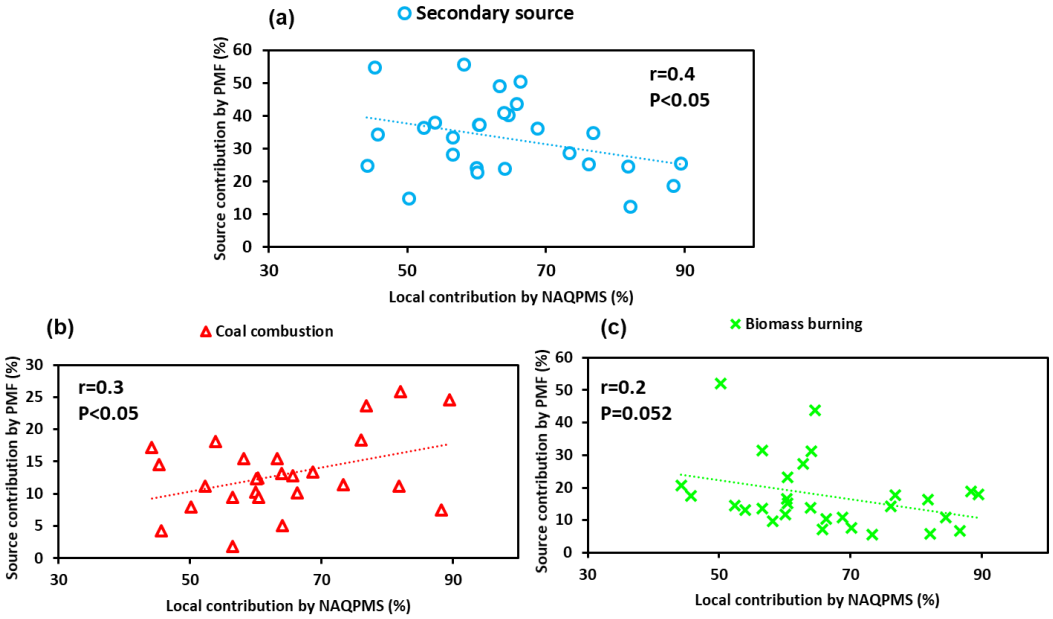

Figure 8. Correlations of local contribution by NAQPMS with the relative contribution by PMF of (a) secondary source, (b) coal combustion source and (c) biomass burning source.

735

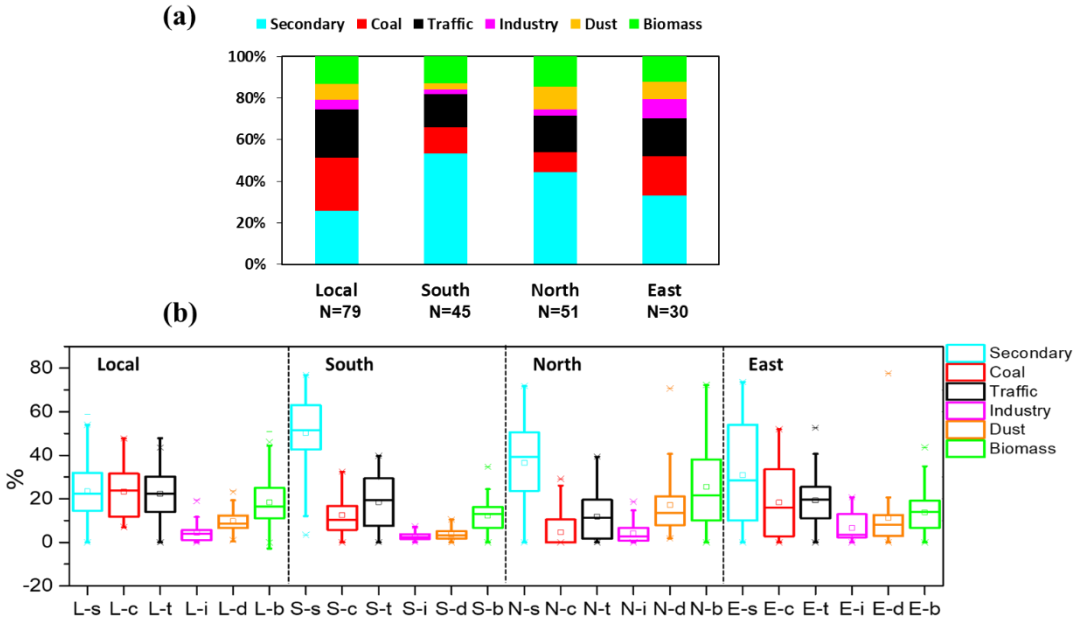

Figure 9. (a) The average source contribution (in percentage) for each type of footprint, and (b) box chart of source contribution in four types of footprint during the whole sampling period. N in (a) represents for the number of cases. The capital letters in (b) stands for the type of footprint (L for local; S for south; N for north; E for east) and the lowercases stands for different sources (s for secondary source, c for coal combustion, t for traffic source, i for industrial source, d for dust, and b for biomass burning)